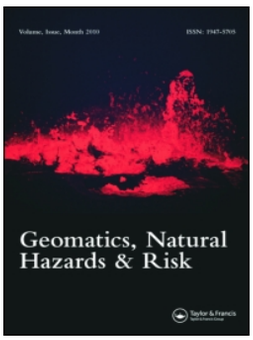

Taylor & Francis
Taylor & Francis Group

Geomatics, Natural Hazards and Risk

ISSN: 1947-5705 (Print) 1947-5713 (Online) Journal homepage: https://www.tandfonline.com/loi/tgnh20

Modelling risk hurricane elements in potentially affected areas by a GIS system

Andrea Taramelli , Laura Melelli , Massimiliano Pasqui & Alessandro Sorichetta

To cite this article: Andrea Taramelli , Laura Melelli , Massimiliano Pasqui & Alessandro Sorichetta (2010) Modelling risk hurricane elements in potentially affected areas by a GIS system, Geomatics, Natural Hazards and Risk, 1:4, 349-373, DOI: 10.1080/19475705.2010.532972

To link to this article: https://doi.org/10.1080/19475705.2010.532972

Geomatics, Natural Hazards and Risk
Vol. 1, No. 4, December 2010, 349–373

Taylor & Francis
Taylor & Francis Group

Modelling risk hurricane elements in potentially affected areas by a GIS system

ANDREA TARAMELLI*†, LAURA MELELLI‡, MASSIMILIANO PASQUI§ and ALESSANDRO SORICHETTA¶

†ISPRA, Institute for Environmental Research, via di Casalotti, 300, Roma, 00166, Italy
‡Department of Earth Science, University of Perugia, 0122, Italy
§Institute of Biometeorology – National Research Council, Firenze, 50145, Italy
¶Dipartimento di Scienze della Terra 'Ardito Desio', Università degli Studi di Milano, 20133, Italy

(*Received 17 June 2010; in final form 18 August 2010*)

In the last decade, modelling hurricanes in potentially affected areas using geographical information systems (GIS) and geospatial cyberinfrastracture (GCI) has become a major topic of research. Despite some basic approaches, some unsolved questions are still under discussion. The disastrous effects of hurricanes on communities are well known, however there is a need to better understand the hazard contributions of the different components related to a hurricane, such as storm surges, floods and high winds. In this paper, the selected approach is to determine an onset zoning from a set of attributes that are considered to govern the hurricane while examining the influence of each individual component that produces the final exposure. To this end, this study assesses the different components using parameters derived from topography, bathymetry and hurricane physical indexes. Key attributes are the river network, the topography, the wetness index and the offline bathymetry. Complementary data include the CMORPH rain dataset and the hurricane track together with its structure model, both based on National Oceanic and Atmospheric Administration (NOAA) datasets. Total hazard results were then overlaid with population data in the overall assessment of elements at risk. The approach, which made use of a number of available global and free datasets, was then validated on a regional basis using ground data collected by the World Food Programme (WFP) over the study area (Central America region) for a specific hurricane.

1. Introduction

The methodology for developing natural hazards is based upon a process by which the hazard can be classified into different phenomena, determined by their geomorphological characteristics and their sensitivity to forcing factors (Melelli and Taramelli 2004, McInnes 2006). As complex physical phenomena they are represented by nonlinear differential equations that can be linearized for the purpose of stability analysis of a system (Taylor 1950, Emmons *et al.* 2006). Basically, the exponential function representing a natural environment could increase infinitely

*Corresponding author. Email: andrea.taramelli@isprambiente.it

Geomatics, Natural Hazards and Risk
ISSN 1947-5705 Print/ISSN 1947-5713 Online © 2010 Taylor & Francis
http://www.tandf.co.uk/journals
DOI: 10.1080/19475705.2010.532972

leading to a hazard situation (Scheidegger 1994). The main issue is that the linearization holds true only for short time ranges so that an unstable state does not necessarily lead to a catastrophe. The growth process, in fact, could come to a stop when a saturation stage is reached so the hazard event could vary greatly in magnitude and frequency. In this context one of the main questions is that the apparent increase in frequency of a natural disaster must be supported by an observation period much longer than a century (Alcantara-Ayala 2002, Alexander 2006) while the consistent reporting of most disaster types has a much shorter history (McInnes *et al*. 2000).

In recognition of this weak understanding in the multi-hazard research (Klein *et al*. 2004, Cecchini 2006, Bell and Tobin 2007), it has often been addressed that a considerable improvement in expertise is necessary in process studies and in mapping of precursor and antecedent conditions of natural phenomena (Hayden *et al*. 2007, Pender and Neelz 2007). Multi-hazard research development has always called for better application of current information technologies, such as geographical information systems (GIS), remote sensing in natural hazard reduction (Alcantara-Ayala 2002, Sorensen 2000, Zenger *et al*. 2002, Zenger and Smith 2003) and geospatial cyberinfrastracture (GCI) (Cruz *et al*. 2007, Ledford 2009, Yang *et al*. 2010, de Longueville 2010). While satellite remote sensing has become a routine tool for land surface classification and mapping (Bocco *et al*. 2001, van Lynden and Mantel 2001), the more recent fusion of these methods with GIS marked a catalytic change in our approach to natural hazard data collection (Burrough 2001, Sanyal and Lu 2004, Yuan 2005). In particular GCI has made the task of managing spatial data much easier, more interactive and informative (Agrawal *et al*. 2006). The advent and evolution of spatial data in the format of GCI provides significant improvements to different geospatial platforms to be used in a first attempt of early warning (Blecic *et al*. 2009). Basically geosimulation modelling entering its age of maturity, the growing computational capabilities of hardware and the consolidation of a GIS-based geo-analysis tool offer the opportunity to foster the development of a robust and scalable early-warning purpose modelling tool (Cattani and Scalia 2009). In this context the role of remote sensing has increased both in the frequency of its use and in its influence upon the monitoring of large natural hazard events (Saito *et al*. 2004, Stramondo *et al*. 2007, Marghany 2009, Taramelli and Melelli 2009a). A growing number of studies have successfully utilized remote sensing to monitor Earth process activity, and subsequently have concentrated on large scale investigations of hazard areas providing hazard zoning maps, or processing studies to assist in structural mitigation (Carson and Arthur 2000, Taramelli and Melelli 2009b, Pasqui *et al*. 2010).

In the last decade, developing hazard models for hurricane impact using GIS and remotely sensed data has become a major topic of research (Colby *et al*. 2000, Guzman-Tapia *et al*. 2005, Taramelli and Melelli 2007). A basic approach based on the multi-hazard model method has been applied to hurricane hazard/elements at risk assessment using GIS data (Boyd *et al*. 2002, Applied Research Associates 2003, Bausch 2003). Indeed, despite the disastrous effects of hurricanes on coastal and inland communities being well known (O'Hare 2001, Pielke *et al*. 2003, Watson and Johnson 2005), there is still a need to better understand the hazard contributions of the different mechanisms related to hurricane strikes, such as storm surges, floods and high winds. However, hurricane hazard areal identification and prediction of their risk assessment remain largely unsolved problems (Kok and Winograd 2002). It

is well known that hurricane hazards are controlled by or dependent on a large and complex set of natural and human induced environmental factors (Howard *et al.* 2003, Shen *et al.* 2005, Pielke *et al.* 2008). To complicate matters further, hurricane related components such as storm surges, floods and high winds, require forecasting appraisal that is often founded upon different methods, techniques and tools (Jiang *et al.* 2003, Bao *et al.* 2006). There is a general agreement among atmospheric scientists that a warmer world would be a wetter world, with no increase in the number of days with rain, but with more intense rainfall (Saunders 1998, Russel *et al.* 2000). This could generate extreme rainstorms that often can be related to hurricane events (Kerry 2005, Webster *et al.* 2005, Pielke *et al.* 2005, Trenberth and Shea 2006). Furthermore, in a recent review paper an extensive analysis of detection, attribution and projection assessments of tropical cyclones changes were proposed by Knutson *et al.* (2010). This paper reviews the existent limitations on the possible attributions of past changes but also the consistent shift, within the future climate scenarios, of globally averaged intensity of tropical cyclones towards stronger storms. Whether tropical cyclone frequency it is likely expected to decrease or remain unchanged, even with a large heterogeneity among basins, intensity and rainfall are expected to increase (Knutson *et al.* 2010). Coastal vulnerability is thus generally expected to increase in a future climate scenario simulation. Unfortunately, there is still a low level of confidence present for future projections of specific storm characteristics that cause hurricane hazards, such as rainfall, high winds and storm-surge floods. Therefore, this kind of situation calls for a multidisciplinary and integrated approach. Technologies such as GIS and remote sensing have raised great expectations as potential means of coping with natural disasters such as hurricanes (Shipley 2005).

This research is part of a service agreement between the University of Perugia and the United Nations World Food Programme (WFP) for developing a Multi-Hazard Assessment Tool for hurricane hazard assessment in Central America. The research made use of a number of available remotely sensed global datasets in order to satisfy the WFP requirement of free and up-to-date datasets. Moreover, datasets that satisfy these characteristics are often the only data available for developing countries such as the ones involved in the WFP activity.

2. Description of the study area

2.1 *The West Indies and Central America*

The West Indies (Anguilla, Antigua and Barbuda, Aruba, Barbados, British Virgin Islands, Bonaire, Cayman Islands, Cuba, Dominica, Curacao, Grenada, Guadeloupe, Dominican Republic, Haiti, Jamaica, Martinique, Montserrat, Netherlands Antilles, Puerto Rico, Saint Kitts and Nevis, Saint Lucia, Saint Martin, Saint Vincent and the Grenadines, Trinidad and Tobago, United States Virgin Islands) and Central America (Guatemala, El Salvador, Honduras, Nicaragua, Costa Rica, and Panama), selected as the study area, are roughly located at latitude 0° S and 30° N and longitude 60° E and 110° W (figure 1).

The study area is a subplate presently attached to the South American plate (Freeland and Dietz 1971) where natural hazards are generally related to deep geology, as recently seen with the Haiti Earthquake (Lin *et al.* 2010) and to hurricanes, especially in the northern and eastern parts of the region due to the

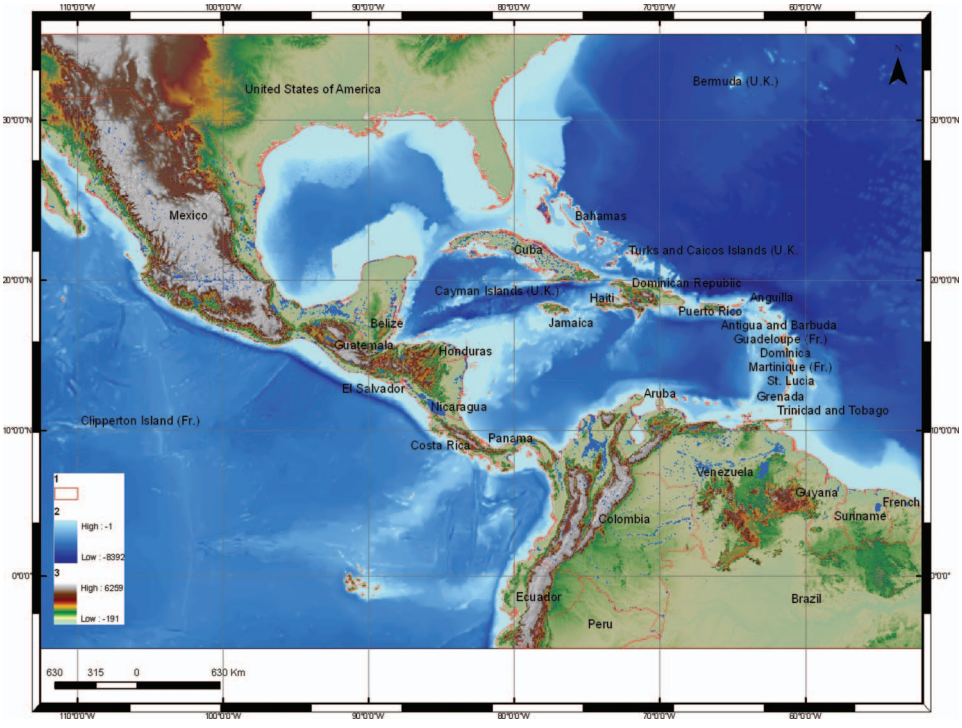

Figure 1. Location map of the study area: (1) country boundaries; (2) GEBCO bathymetry, (3) SRTM digital elevation model.

geographic location (Palmieri *et al.* 2006). Although largely similar in climatic and biophysical characteristics (Schumann and Partridge 1989), the study area displays large economic (World Bank 1998), environmental and political (Pelupessy 1991) differences. Especially biophysical, climatic, and socioeconomic gradients (mountain ranges, rainfall and population density) are steep over small distances within the countries, which induce strong variation in land-use over relatively small areas.

2.2 *Climatic background*

Climate in the Caribbean basin can be classified as dry-winter tropical, with significant subregional variations in rainfall annual totals, length of the rainy season, and timing of rainfall maxima. The climatologic (1951–1980) annual mean rainfall, averaged over all the 188 stations (Giannini *et al.* 2000), is 1618 mm per year. It exceeds 2000 mm per year in Costa Rica and along the Caribbean coast of Honduras. Three rainfall regimes can be related to the geography of the Caribbean-Central American region. A May–October rainfall regime is typical of the Central American region. A regime characterized by a pronounced midsummer break in rainfall accumulations is typical of the interior of the basin (southern coasts of Jamaica and Hispaniola). A regime characterized by a late-fall peak in rainfall is typical of the Caribbean coast of Honduras, of the northern coasts of Jamaica and Hispaniola, of Puerto Rico and of the Lesser Antilles. In this context rainfall-bearing disturbances, known as African easterly waves (Riehl 1954, Burpee 1972), propagate across the Atlantic Ocean into the Caribbean basin from mid June to early October, generating hurricanes.

3. Data source

3.1 *Hazard assessment*

The multi-hazard model includes a large volume of resident GIS-readable databases, including physiographic data relating to terrain (i.e. land cover), topography, and inventory data pertaining to population density. These datasets include worldwide data on bathymetry physical characteristic as well as rain density data.

3.1.1 Topography dataset. The Shuttle Radar Topography Mission (SRTM) data, characterized by a recent and extensive literature (Farr *et al.* 2007 and references within), is available at http://seamless.usgs.gov. In this analysis we have used the SRTM data version 2. The SRTM data in their original format have a resolution of 3-arc-seconds, corresponding approximately to 90 m × 90 m over the study area. Assemblage and local interpolation of the SRTM was performed importing tiles into ArcInfo 9.x (©ESRI) using an Arc-Macro Language procedure (Taramelli and Barbour 2006).

3.1.2 Bathymetry dataset. The GEBCO One Minute Grid (Jones 2003) is global and includes land elevations from the IGBP GLOBE database (figure 1). A medium stage bathymetry dataset, exported from GEBCO with a 1 km horizontal resolution, was examined in Interactive Visualization Systems software for further cleaning, geomorphic analysis, and exporting grids to ArcMap GIS. Resolution of the bathymetry data was such that landscape features and differences of the order of 1 km horizontal were clearly discernable. Data were rigorously edited for spurious points and smoothed and gridded to 1- km intervals to minimize data gaps in the final xyz export. The net vertical resolution was multiplied by the single pixel area (90 m × 90 m) and re-interpolated to arrive at the net value in all areas of the bathymetry.

3.1.3 Rain dataset. The Climate Prediction Center Morphing Method (CMORPH) uses motion vectors derived from half-hourly interval geostationary satellite InfraRed imagery to propagate the relatively high quality precipitation estimates derived from passive microwave data. In addition, the shape and intensity of the precipitation features are modified (morphed) during the time between microwave sensor scans by performing a time-weighted linear interpolation (Levizzani and Mugnai 2004, Joyce and Ferraro 2005).

The hourly analyses of CMORPH at a grid resolution of 1 km have been produced using the INGRID programme at the IRI/LDEO Climate data library website (http://ingrid.ldeo.columbia.edu/). The INGRID is an alternative mesh generator for finite element modelling, which is principally used as a fairly complete mesh generator with a wide range of geometric capabilities.

3.1.4 Winds dataset. The National Hurricane Center's Tropical Cyclone Reports contain comprehensive information on each tropical cyclone, including synoptic history, meteorological statistics, casualties and damage, and the post-analysis best track (6-hourly positions and intensities). These data are of key-importance in vulnerability assessment. The lessons learnt in past events can really help to strengthen prospective scenarios. Tropical cyclones include depressions, storms and hurricanes (Abraham *et al.* 2004). In particular, the report was used to calculate the standard temperature and pressure R0 following the axisymmetric hurricane wind model from

Holland (1980). It assumes that for a generic tropical cyclone, the surface pressure field follows a modified rectangular hyperbola, as a function of radius in the cyclostrophic balance. Even if the axisymmetric is rare, it is possible to introduce deviation from that geometry in a simple way: for example dividing the wind fields into quadrants. Following the idea proposed in Bao *et al*. (2006) we computed the wind field, for each single quadrant, from the maximum sustained wind observed (Xie *et al*. 2006) and reported in the NHC website (http://www.nhc.noaa.gov" > http://seamless.usgs.gov. In this analysis we have used the SRTM data version 2. The SRTM data in their original format have a resolution of 3-arc-seconds, corresponding approximately to 90 m × 90 m over the study area. Assemblage and local interpolation of the SRTM was performed importing tiles into ArcInfo 9.x (©ESRI) using an Arc-Macro Language procedure (Taramelli and Barbour 2006).

3.1.2 Bathymetry dataset. The GEBCO One Minute Grid (Jones 2003) is global and includes land elevations from the IGBP GLOBE database (figure 1). A medium stage bathymetry dataset, exported from GEBCO with a 1 km horizontal resolution, was examined in Interactive Visualization Systems software for further cleaning, geomorphic analysis, and exporting grids to ArcMap GIS. Resolution of the bathymetry data was such that landscape features and differences of the order of 1 km horizontal were clearly discernable. Data were rigorously edited for spurious points and smoothed and gridded to 1- km intervals to minimize data gaps in the final xyz export. The net vertical resolution was multiplied by the single pixel area (90 m × 90 m) and re-interpolated to arrive at the net value in all areas of the bathymetry.

3.1.3 Rain dataset. The Climate Prediction Center Morphing Method (CMORPH) uses motion vectors derived from half-hourly interval geostationary satellite InfraRed imagery to propagate the relatively high quality precipitation estimates derived from passive microwave data. In addition, the shape and intensity of the precipitation features are modified (morphed) during the time between microwave sensor scans by performing a time-weighted linear interpolation (Levizzani and Mugnai 2004, Joyce and Ferraro 2005).

The hourly analyses of CMORPH at a grid resolution of 1 km have been produced using the INGRID programme at the IRI/LDEO Climate data library website (http://ingrid.ldeo.columbia.edu/). The INGRID is an alternative mesh generator for finite element modelling, which is principally used as a fairly complete mesh generator with a wide range of geometric capabilities.

3.1.4 Winds dataset. The National Hurricane Center's Tropical Cyclone Reports contain comprehensive information on each tropical cyclone, including synoptic history, meteorological statistics, casualties and damage, and the post-analysis best track (6-hourly positions and intensities). These data are of key-importance in vulnerability assessment. The lessons learnt in past events can really help to strengthen prospective scenarios. Tropical cyclones include depressions, storms and hurricanes (Abraham *et al*. 2004). In particular the report was used to calculate the standard temperature and pressure R0 following the axisymmetric hurricane wind model from Holland (1980). It assumes that for a generic tropical cyclone, the surface pressure field follows a modified rectangular hyperbola, as a function of radius in the cyclostrophic balance. Even if the axisymmetric is rare, it is possible to

introduce deviation from that geometry in a simple way: for example dividing the wind fields into quadrants. Following the idea proposed in Bao *et al.* (2006) we computed the wind field, for each single quadrant, from the maximum sustained wind observed (Xie *et al.* 2006) and reported in the NHC website (http://www.nhc.noaa.gov).

3.2 *Elements at risk*

3.2.1 Land cover dataset. The Global Land Cover database is being produced by an international partnership (Hansen *et al.* 2000). The database contains a global product that combines all regional classes in one consistent legend (Mucher and Badts 2002). To create the final landcover dataset of the study area a reclassification of the different landcover classes was carried out. We decided to use the decision trees approach due to the numerous classes in the landcover dataset (21). Some of them could be clustered within the same class (e.g. shrub cover with herbaceous cover). Decision trees provide a more rational approach to land cover classification than traditional statistically supervised classification. Decision trees allow the user to specify the exact logical basis of class assignment in the form of a Boolean condition of arbitrary complexity. So as final classes we have: tree cover, regularly flooded shrub, cultivated and managed areas, cropland, bare areas, water, artificial surfaces and associated areas and irrigated agriculture (figure 2).

3.2.2 Population dataset. Affected populations are assessed on a $2.5' \times 2.5'$ latitude-longitude grid of global population, the Gridded Population of the World, version 3 (GPWv3). The GPWv3 depicts the distribution of human population across the globe transforming population census data (corresponding to irregularly vector census block and block group boundaries), which most countries collect for subnational administrative units, into a regular raster-grid. Each cell contains an estimate of total population and population density on land, based on the overlap between the irregular boundaries of administrative units and the regular boundaries of the grid. In this analysis (figure 3), we used a preliminary version of GPWv3, which contains population estimates for 1990, 1995, and 2000 for approximately 375,000 sub-national administrative units (Center for International Earth Science Information Network *et al.* 2004).

4. The Stan event on the Caribbean area

A tropical wave that moved off the coast of Africa on 17 September 2005 was the likely precursor to Stan (figure 4).

Cloudiness and showers associated with the system began to increase as the wave neared 50° W longitudes on 22 September but a north-north-easterly shear created an environment that was not favourable for tropical cyclone formation. The wave moved into the eastern Caribbean Sea on 25 September, while a shear over the system diminished. By 27 September, deep convection associated with the wave became more consolidated over the central Caribbean Sea. Based on the extent and organization of deep convection as well as surface observations, it is estimated that a tropical depression formed around 12.00 UTC on 1 October centred about 115 nmi southeast of Cozumel. Lower to middle-tropospheric ridging to the north and northeast of the tropical cyclone resulted in a west-north-westward steering current

Figure 2. Land cover map of the study area: (1) country boundaries, (2) tree cover – evergreen, (3) tree cover – deciduous closed, (4) tree cover – deciduous open, (5) tree cover – needle leaved, (6) tree cover mixed leaf type, (7) tree cover regularly flooded fresh water, (8) tree cover regularly flooded saline water, (9) tree cover/other natural vegetation, (10) shrub cover closed-open evergreen, (11) shrub cover closed-open deciduous, (12) herbaceous cover, (13) sparse herbaceous or sparse shrub cover, (14) regularly flooded shrub and herbaceous cover, (15) cultivated and managed areas, (16) cropland, (17) tree cover and other natural vegetation, (18) cropland, shrub and grass cover, (19) bare areas, (20) water, (21) snow and ice, (22) artificial and associated areas, (23) irrigated agriculture.

and an upper-tropospheric anticyclone became established over the area. The depression strengthened into a tropical storm shortly before its centre made landfall on the east coast of the Yucatan peninsula, just south of Tulum, around 10.00 UTC on 2 October. Stan crossed the peninsula in about 18 hours while weakening back to a depression. It quickly regained tropical storm strength, however, after it moved back over water. Deep layer high pressure over the western Gulf of Mexico forced the system to turn towards the west-southwest over the Bay of Campeche. As Stan approached the southern Gulf coast of Mexico, it rapidly intensified into a hurricane around 06.00 UTC on 4 October. The most affected countries were Guatemala, El Salvador, Mexico (its southern and eastern parts), Nicaragua, Honduras and Costa Rica.

5. Methodology

In this research the major constraint in using GIS (ArcGis 9.3 ©) to evaluate hurricane hazards is the complexity of the hazard-generating phenomena. Moreover hurricane hazards are the result of the interaction of both internal factors such as

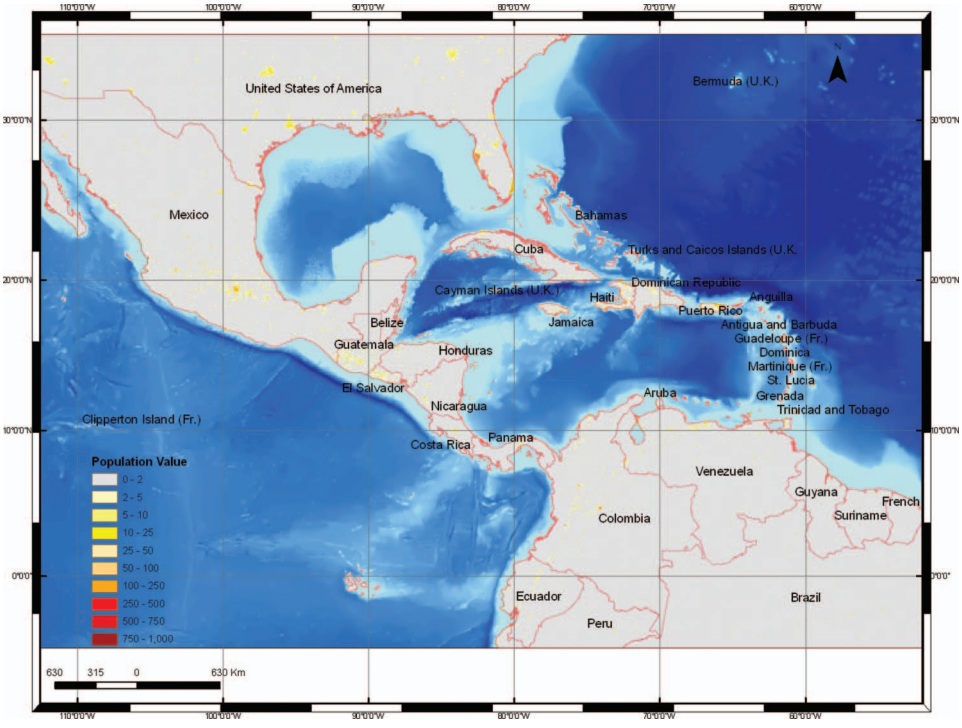

Figure 3. Estimate of total population and population density of the study area.

topography, bathymetry and hydrology, and external factors, such as high winds and precipitation (Taramelli and Melelli 2007). The key issue in forecasting the hurricane hazards is the identification and collection of the relevant predictors whose nature, character and role will vary depending on the type of hurricane and on the geomorphologic and climatic setting of the region affected by the hurricane itself. The steps to build the final structure of the hurricane multi-hazard GIS model presented in this research are (figure 5):

(1) georeferentiation of the location sites and their spatial attributes (topography, bathymetry and precipitation);
(2) modelization of the hurricane hazard related to three different components such as storm surges, high winds and floods;
(3) examination of the spatial distribution of the hurricane hazard;
(4) assessment of the elements at risk to be potentially affected by the components (overlay analysis with the land cover and population dataset).

The major concern in the modelling implementation was the use of ArcGis 9.3© as it is not an open source. We ended up using this software based on a specific request of the WFP, which was already using the software infrastructure.

5.1 *Storm surges*

Storm surges are oscillations of the water level in a water body having a period ranging from a few minutes to a few days, associated with a low pressure weather

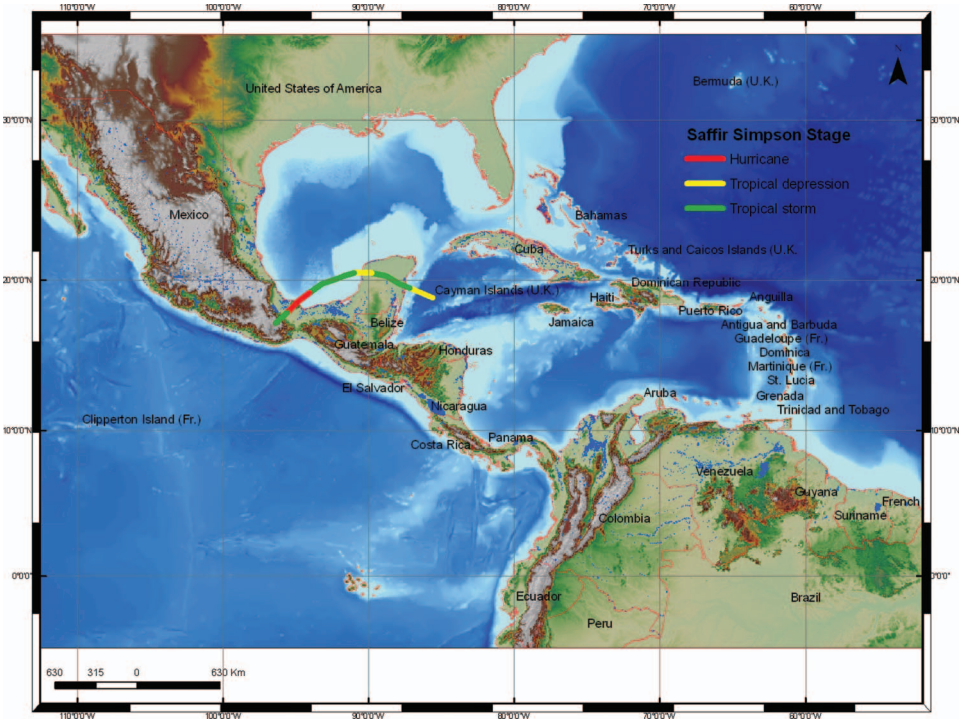

Figure 4. Hurricane track of the Stan event.

system (Blain 1997, Gonnert *et al.* 2001). Although storm surges belong to the same class known as long gravity waves, as do tides and tsunamis, there are at least two important differences. First, whereas tides and tsunamis occur on the oceanic scale, storm surges are simply coastal phenomena. Second, a storm surge is defined as an abnormal, sudden rise of sea level associated with a storm event. Storm surges result from the combination of low barometric pressure, strong onshore winds and higher than normal tides (Goring 1999). Most commonly, storm surge elevation of sea level occurs in response to a decrease in atmospheric pressure, to an increase in wind stress on the surface of the ocean and to the slope of the bathymetry and of the coast. Due to this fact, storm surge is generally constant over a large area (Munro 1999).

The model implemented in this project calculates the proportional height of the bathymetry near the coast line and consequently the hazard degree value onshore related to the slope angle of the topography (figure 6).

The storm surge was calculated using a SRTM digital evaluation model (DEM) and GEBCO Dataset in ArcGIS 9.x software (ESRI©). The analysis was cast in different steps:

(i) the coastline was modelled as a polyline for the study area using the National Oceanic and Atmospheric Administration (NOAA)/National Ocean Service (NOS) Medium Resolution Coastline designed for 1:70,000 (available at: http://www.ngdc.noaa.gov/mgg/shorelines/shorelines.html);

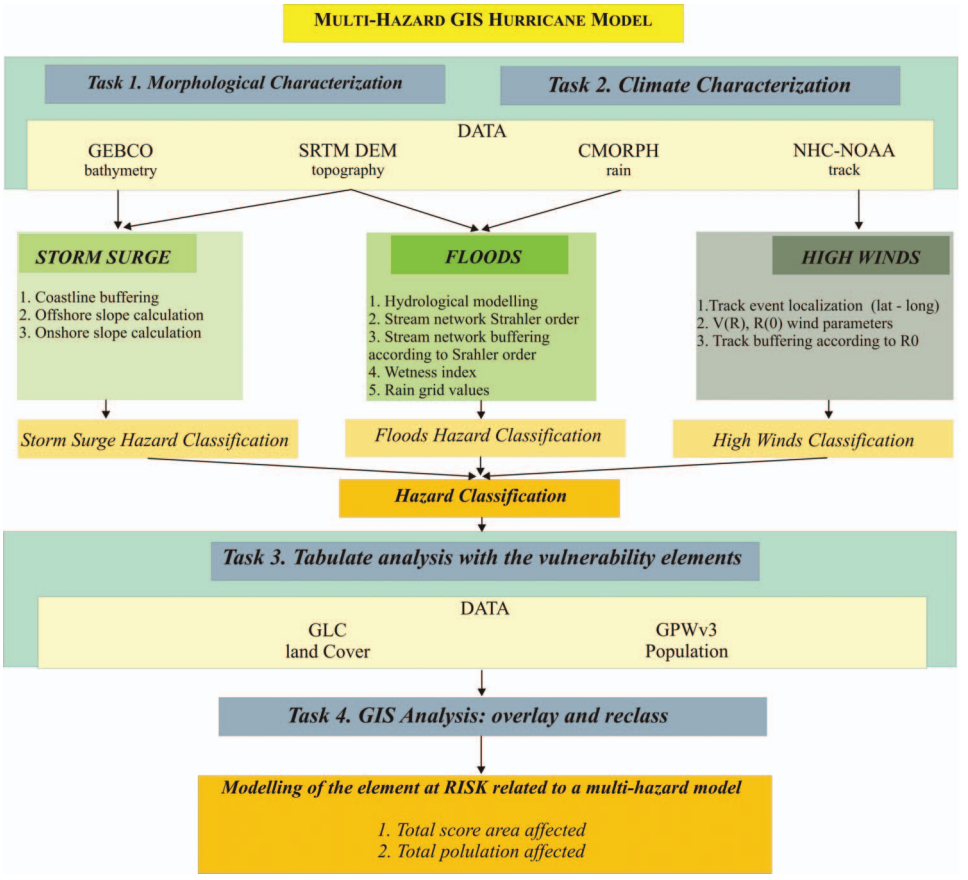

Figure 5. Flow chart of the GIS hurricane early warning model.

(ii) based on literature data (Blain *et al*. 1997, 1998, Zenger *et al*. 2002) a 5 km width buffer was calculated around the coastline for the far reachable distance value onshore;

(iii) for both onshore and offshore, potentially affected area slope grids were calculated respectively from SRTM, GEBCO datasets.

(iv) Both slope grids were reclassified in three increasing storm surge hazard classes (from value 1, minimum hazard to value 3, maximum hazard) based on the proportional height of the bathymetry near the coastline related to the slope angle of the topography (figure 6).

(v) Finally, we produced a final storm surge hazard assessment identifying every grid node, within the 5 km coastline buffer area, having the three different hazard values. The resulting grid (see figure 7) shows values that vary from 1 to 3, indicating respectively the greatest, the medium and the lowest likelihood of hazard signatures.

For the Stan event (figure 7(*a*)) the potentially affected area is around 36 km^2 whereas the potentially affected population is near 22 524 persons. Figure 7(*b*) shows the distribution of the areas and the population in the three storm surge hazard classes.

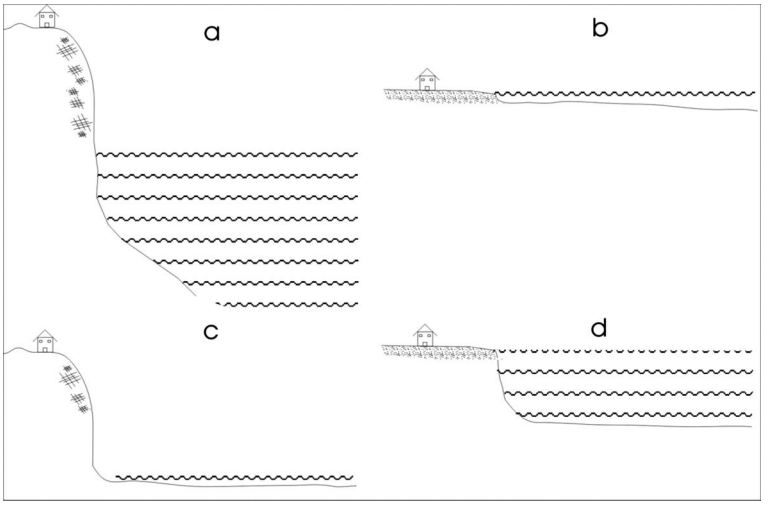

Figure 6. (*a*) Low hazard degree with high slope angle and deep water, (*b*) high hazard degree with low slope angle and shallow water, (*c*)–(*d*) medium hazard degree with medium slope angle/shallow-medium deep water.

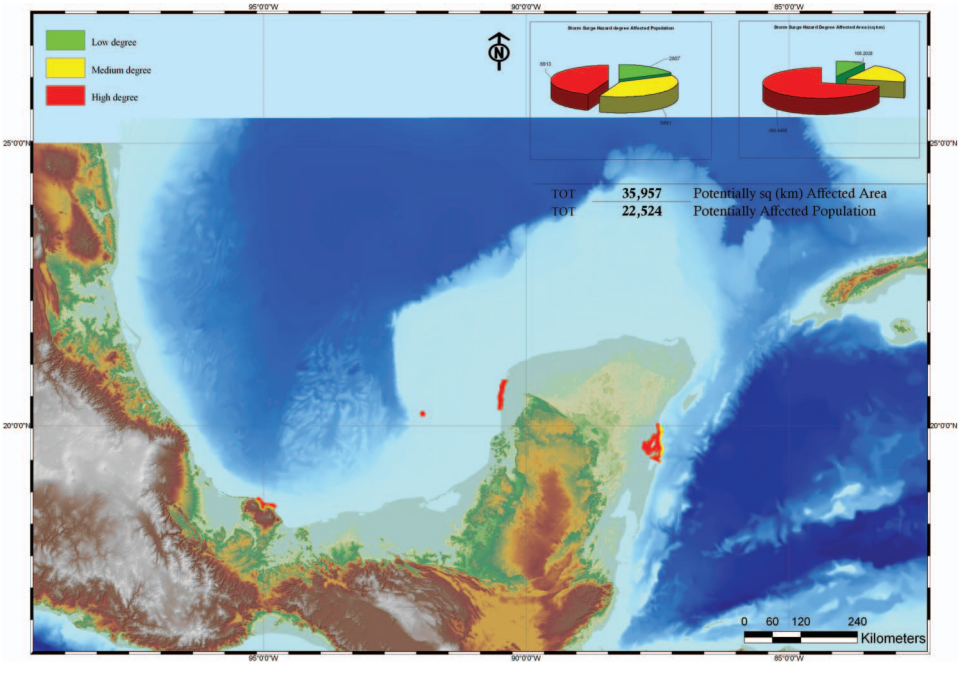

Figure 7. Storm surge hazard assessment related to the Stan hurricane event. Inserts showing storm surge affected population of the study area and storm surge affected area.

5.2 *Floods*

A flood related to a hurricane event occurs when a stream overflows after prolonged intense rainfall over several days. The intensity of a flood varies widely from one site to another because of local conditions. A simple representation of flood affected

areas in a way that is easily grasped by the early warning managers, but still accurate and scientifically sound, is an important product of a flood study. With this concern in mind, there is much to gain in coupling the traditional and cumbersome hydrologic modelling with advanced and sophisticated computer tools within GIS. Hydrologic modelling deals frequently and extensively with spatial data. Input, parameters and output are space-time defined. In this context different studies (Tucker *et al*. 2000, Tarboton and Ames 2001, Hancock and Evans 2004) investigate the flood modelling through the use of Digital Elevation Models (DEMs). In this research the most important variables relevant to flood hazard assessment are: meteorological data (rainfall depths and intensities, magnitude and frequency of rain peak) and topographic data of the catchment basins struck by the hurricane. Due to spatial data integration issues within GIS, such as geographical scales of the study area, the geologic factors such as permeability and soil type are not taken into account. The final flood hazard analysis was cast in different steps using ArcGIS 9.x software (ESRI©):

(1) The delineation of the flow direction grid is carried out exploiting the eight-direction pour point model (Puecker and Douglas 1975).
(2) The method of Jenson and Domingue (1988) is used to determine the flow accumulation grid.
(3) The stream network in a grid structure is then derived.
(4) The stream network is classified according to the Strahler method (Strahler 1980) assigning a numeric order to links in a stream network based upon their number of tributaries. For the study area according to previous studies (Correia *et al*. 1998, Colby *et al*. 2000, Taramelli and Melelli 2007) the fourth order is the maximum value assigned.
(5) The river network grid is converted in a vector layer (polyline) and then a buffering is made in order to link the stream order to a potential affected flooded area considering a linear proportional relation between the two variables. Based on the literature (Penning-Rowsell and Fordham 1994, Penning-Rowsell 1996, Correia *et al*. 1998) a buffering width equal to 200 m is measured for the first order, 1000 m for the second, 2000 m for the third and 4000 m for the fourth. Then the buffer layers area is converted to a grid format with the river order value assigned to each pixel.
(6) The wetness index is calculated using the Terrain Analysis Digital Elevation Model (TauDEM) plug-in (Tarboton 1998, Tarboton and Ames 2001) in order to consider into the hydrologic model the topographic parameter of the flooding areas. This calculation estimates the ratio slope/catchment area, where a specific catchment area is the ratio between a contributing area concerning a specific unit contour length along the slope. This is algebraically related to the more common wetness index, with the contributing area at the denominator to avoid errors dividing by 0 when the slope value is 0° (Costa-Cabral and Burges 1994, Tarboton 1998).
(7) The wetness index grid is reclassified in three increasing hazard degree classes (Speight 1984, Taramelli *et al*. 2008). This grid relies on topographic variables only and it is still independent from specific rain values.
(8) A CMORPH rain dataset for the specific Stan hurricane event (between 1 and 5 October 2005) is calculated by the INGRID mesh generator. It is

interesting to note that high rain values are present not only near the hurricane track but also far away from the eye of the event due to the topography of the test area.

The total rain values grid is then overlaid on the wetness index achieving the final flooding hazard grid. Each area is zoned in terms of degree of hazard and each zone is classed as low flooding, medium flooding and high flooding and allocated the numeric values 1, 2 and 3, respectively. We produced a final flooding hazard assessment identifying every grid node within the zones having only three different hazard values that fall within the sum of evidence criteria using the reclassify operator in a GIS environment. The resulting grid shows values that vary from 1 to 3, indicating respectively the lowest, the medium and the greatest likelihood of hazard signatures (figure 8).

For the Stan event (figure 8(*a*)) the potentially affected area is around 321 km^2 whereas the potentially affected population is near 8,500 persons. Figure 8(*b*) shows the distribution of the areas and the population in the three flooding hazard classes.

5.3 *High winds*

Another key variable in the hurricane hazard is the estimate of the area struck by the high winds. In the absence of detailed instrument observations we assumed that wind velocity increases linearly from the centre to the outer side (Holland 1980, Holweg 2000) and thereafter decreases exponentially moving outwards. Moreover, the

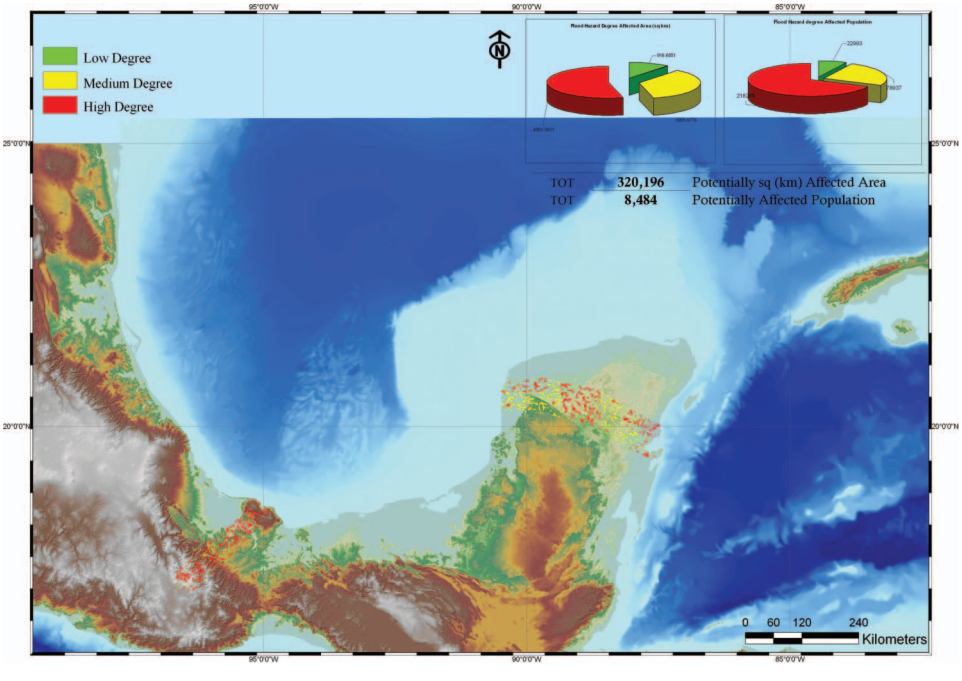

Figure 8. Flooding hazard assessment related to the Stan hurricane event. The assessment of the rain-rate is within the watershed area using cumulate values. (*a*) Flooding affected population of the study area, (*b*) flooding affected area.

horizontal wind field is asymmetrical and, in the northern hemisphere, the strongest winds are found in the right-hand quadrants of the storm (relative to the direction of movement) due to the Coriolis force.

Based on the aforesaid basic model, in this study we used the NOAA preliminary hurricane report (Pasch and Roberts 2006, Xie *et al*. 2006) in order to gain all the comprehensive information on each hurricane, including synoptic history, meteorological statistics and the post-analysis best track (6-hourly positions and intensities). The track and the intensity evolution (from NHC) of hurricane Stan, shown in figure 4, are the first inputs to the model as latitute-longitude point features. Then the term intensity evolution of the hurricane event is referred to the temporal variation of the R0 while changes in near-eye wind mean velocity, near-eye diameter, atmospheric pressure are documented to check whether the models storm evolve (Xie *et al*. 2006). In order to estimate the potentially affected areas by high winds we worked through a processing sequence:

(i) first we imported the latitude-longitude text file from the NOAA preliminary report as the event theme;
(ii) we assessed the cyclone's mean sustained surface wind, based on the radius maximum wind speed and on the pressure within the same radius. The wind at each level of the hurricane has been normalized by the wind speed of the different quadrant based on the asymmetric modelling of the hurricane itself and the V(R) velocity was calculated based on the Holland model for each quadrant and all the model parameters were computed from the hurricane report on the NHC web page (figure 9);
(iii) we evaluated the ratio of the R0 East and R0 West related to the stage of the Saffir-Simpson scale of the Hurricane (Blog 2004). The ratio is 0.8 for the R0 West and 1.2 for the R0 East;
(iv) the two different R0 values were calculated and then joined with the XY event theme to generate a polyline vector file;
(v) a rounded buffer file was created using the two different R0 values leading to the polygon vector file within the value of R0 intensities that represents the intensity evolution of the hurricane event referred to as the temporal variation of the R0;

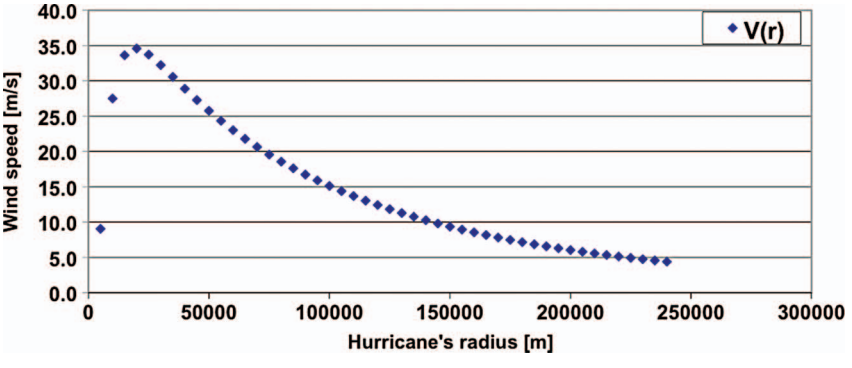

Figure 9. Plot of the V(r) values. X values are the radius of the hurricane track (m); Y values are the V(r) values (m s^{-1}).

(vi) we finally converted the polygon vector file to an integer grid file representing the different hazard values. Values for the resulting dataset, which we term degree values, vary continuously from 1 to 3, with 1 representing terrain with a low hazard degree and 3 indicating that all of the terrain exhibits a high hazard degree (figure 10).

As a preliminary result, it can be noticed that the high values of the signature are shown in red, medium values in yellow and low values in light green. As can be seen, in addition to the relatively homogeneous values near the coastal area, there is a wide variety of different signals throughout the ridge region and a widespread boundary region area of strongly high value composition.

For the Stan event (figure 10(*a*)) the potentially affected area is around 36,000 km^2, whereas the potentially affected population is near 1407 people. Figure 10(*b*) shows the distribution of the areas and the population in the three high wind hazard classes.

As already noticed, for each hazard evaluation the final grid is reclassified into three categories (value 1 for low degree, 2 for medium, 3 for high). The Jenks classification (natural breaks) is applied (Jenks 1967). Classes are selected on natural groupings contained in the data with similar values. The break points are identified where huge jumps in the data sequence are present (Goodchild *et al*. 1992, Osaragi 2002).

6. Discussion

The main objective of our GIS approach was the analysis of the morphogenetic and atmospheric parameters influencing the hurricane effects, for the purpose of

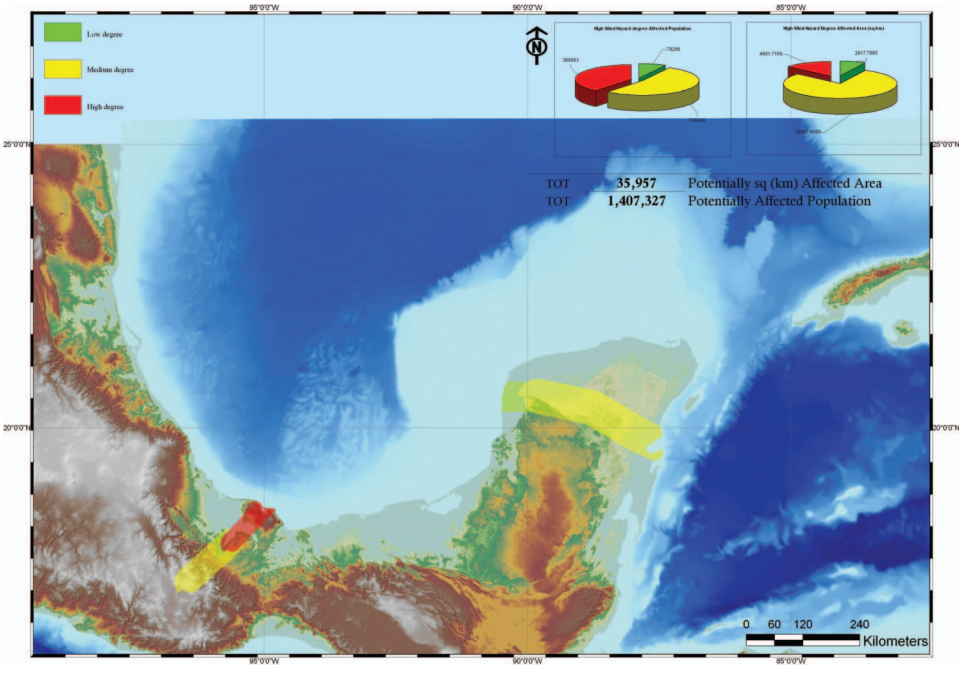

Figure 10. High wind hazard assessment related to the Stan event. Inserts showing high winds affected population of the study area and high winds affected area. Available in colour online.

identifying the key factors for a methodology concerning a multi-hazard model. In order to obtain a final hazard assessment we have first been working on the analysis models to produce:

- areas potentially affected by storm surge
- areas potentially affected by high speed winds
- areas potentially affected by floods.

Each zone was numerically scored and each theme was zoned in terms of degree of hazard. The themes were categorized in terms of low hazard, medium hazard, high hazard and allocated the numeric values 1, 2 and 3, respectively. This process was done with each hazard theme. Finally, based on the single hazard results, we produced a final multi-hazard assessment identifying every grid node within the area having the three different hazard values that fall within the model criteria using the Boolean method (and) overlaid in a GIS environment. This was done in order to consider always each single high hazard degree even if the other two were not happening in the same area. The resulting grid shows values that vary from 1 to 3, indicating the greatest likelihood, the medium and the lowest likelihood of hazard signatures, respectively by 3, 2 and 1. So the final multi-hazard was coded into three classes:

(1) high (all three hazards have a high value),
(2) medium (two of the three hazards have a high value),
(3) low (at least one of the three hazards has a high value).

After that, the elements at risk were evaluated for each hazard zone. The element at risk assessment requires that critical facilities are identified and data on past physical effects, in terms of structural and functional damage be collected. This allows to enquiry the same datasets for each hurricane components, knowing the track and the physical characteristics of the event, obtaining, for each example, the risk evaluation. These data are to be entered into a database and integrated into a GIS. In this research, instead, to assess the overall elements at risk, the hazard results were overlaid only with population and landcover datasets. The approach was then validated on a regional basis using the Stan event report on elements affected by damaging components (OCHA 2005a, b) over an area that covers both developed and developing countries in the Caribbean Region. The reports allow us to know the effects of the Stan event in the study area and to compare the numbers obtained from the model (in terms of affected area and population) to the real effects summarized in the regional reports. So the key layers in the GIS model are to be the hazard maps of high wind, storm surge and floods with the elements at risk spatial layers of features to be included such as agricultural and managed areas and number of population at a pixel scale. The final elements at risk assessment as set out in this research consist of the following:

- identification of the hazard
- creation of the specific elements at risk zone maps
- calculation of a total score of population and total area affected for each single hazard and for the final hazard.

The design of the multi-hazard GIS model seeks to automate the assessment process because it facilitates the conduct of spatial and tabular analysis to calculate the area and population estimation scores (Santini *et al.* 2010). In each hazard area, the hazard boundaries were used to perform a 'tabulate' analysis in each available 'elements at risk' dataset. The 'tabulate' function was used to compute the estimation score using the buffer class of the hurricane track as the polygon mask. On the basis of the different hazard entities determined, three tables were created: high winds, storm surge and flood estimated population. Then once a set of grids has been created on the basis of the three tables, it was possible to calculate link-by-link statistics in with the ZONALSTATS command. The output is an attribute table, which has an entry for every zone. In this research the zone is a grid of the three hazard values and only includes the equation for a population table, the managed and cultivated areas tables, and the human settlements table. A first analysis shows the results of the three different sums of the hazards (figure 11).

The final score of the population and affected area is shown in the tables.

It is important to note that the final affected population and total affected area related to the hurricane Stan final score estimation appeared to be embedded within the western portion of a broader-scale low-level cyclonic circulation. This larger system produced extensive very heavy rains over portions of extreme eastern Mexico and Central America that resulted in disastrous floods. Estimates of the total number of lives lost in Mexico and Central America are mostly in the range of 1000 to 2000, some even higher (OCHA 2005a, b). Guatemala was hit particularly hard and over 1000 persons may have perished in that country alone (UNEP-OCHA 2005). As can be seen, in addition to the relatively homogeneous values of the hazard signature near the coastal area, there is a wide variety of different signals throughout the ridge

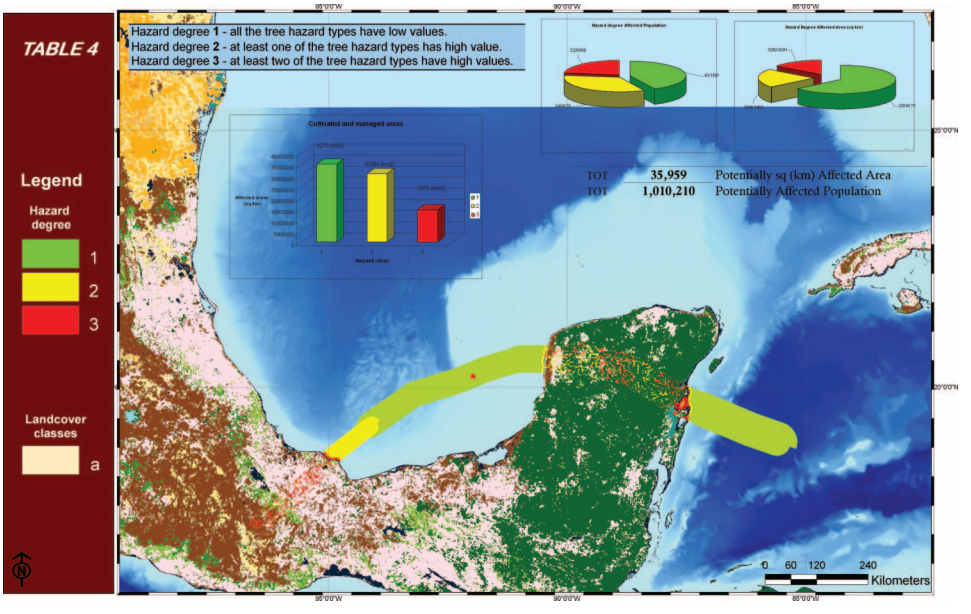

Figure 11. Final overlay of the sum of the three hazards, the gridded population dataset and the land-cover reclassified dataset.

region and a widespread boundary region area of strongly high value composition far away from the hurricane track. This widespread signature confirms the high correlation between the affected population score and the flooding environmental variables, which shows an overestimation score between the affected population and the storm surge hazard, probably due to some weakness in the storm surge modelling such as the non consideration of the impact angle effect.

In order to finally calculate the estimate of the affected population we look at the population living in the potentially affected areas, comparing the data with the land cover use (in this case the cultivated-managed area and artificial surface). To this end, we obtain a final rough estimate of the affected population based on the information available. The number of the potential population is estimated out of a certain percentage, based on the hazard evaluation, out of the population living in the affected area (figure 11).

The multi-hazard GIS model developed for elements at risk assessment produces a mix of tabular and spatial manipulations for specific population estimation scores for critical land cover and specifically for topographic parameters. It can be noticed that topography highlights several high score values throughout areas far from the point where the hurricane makes the landfill. This is a consistent result with a high correlation with the estimated score of the affected population from field reports (figure 11). Although these scores are a measure of relative elements at risk they can be utilized to identify areas with the highest susceptibility to hurricane components.

7. Conclusion

The key result of the research is that understanding the element at risk and the morphological and atmospheric parameters is essential for predicting the response to a hurricane hazard. Earth surface systems in the Central America area provide the framework for developing this understanding, most appropriately at the scale of both coastal behaviour and inland system and to an appropriate morphological and atmospheric scale. The applied model is not only conceptual. It is one of the first attempts to evaluate hazards quantitatively at a regional scale on a physically based model. The study highlights that over time, the morphology of different subsystems represents a balance between inputs (forcing agent) and natural response (related single hazards). Moreover, the morphology (e.g. beach height, wetness index) also influences the available on set zonation. In addition the ArcGIS model describes the morphological response to variations in the balance between the forcing factors (e.g. wind velocity) and one of the related single hazards (e.g. storm surge wave). ArcGIS is able to manage the most interchangeable formats among GIS software and tools. The model could be extended to generate, for example, vector grids of square polygons storing in each feature (cell) the estimated affected population value to be then visualized and used in Google Earth or in other web mapping systems. We have highlighted how such modelling tools have an increasing usefulness for scales ranging from regional to semi-regional, while for local applications often treated with local mapping the modelling system is not so highly reliable.

As a final remark the GIS hurricane model approach shown in this study could be used for different term simulations and it should be considered as a potential monitoring tool in an integrated management approach to hurricane hazard mitigation and control. It is a practical tool for building possible intervention scenarios both for small and large-scale areas, providing, also, quantitative

evaluations of the elements at risk and inter-linkages between the different landforms involved (coastal or in land).

Acknowledgments

The authors are grateful to Francesca Guarnieri for her help in developing the wind model calculation. We would also like to acknowledge the support of Giorgio Sartori within the WFP Service agreement no. SA/2006/08. When this study began, A. Taramelli was affiliated with the Department of Earth Sciences of Perugia University and the LDEO of Columbia University, A. Sorichetta was affiliated with the CUNY Queens College's School of Earth and Environmental Sciences.

References

Abraham, J., Strapp, J.W., Fogarty, C., Wolde, M., 2004, Extratropical transition of hurricane Michael. *American Meteorological Society*, **9**, pp. 1323–1339.

Agrawal, G., Fernhatosmanoglu, H., Niu, X., Bedford, K., Li, R., 2006, A vision for Cyberinfrastructure for coastal forecasting and change analysis. *Lecture Notes in Computer Science*, **4550**, pp. 127–144.

Alcantara-Ayala, I., 2002, Geomorphology, natural hazards, vulnerability and prevention of natural disasters in developing countries. *Geomorphology*, **47**, pp. 107–124.

Alexander, D., 2006, Globalization of disaster: trends, problems and dilemmas. *Journal of International Affairs*, **59**, pp. 1–22.

Applied Research Associates, Inc., National Institute of Building Sciences, and Federal Emergency Management Agency, 2003, Research to Develop Advanced Severe Storm Coastal Risk Assessment Methodology Using NASA's WAVEWATCH III and Remote Sensing Technology. Unsolicited proposal, submitted to NASA 23 April, 34 pp.

Bao, S., Xie, L., Pietrafesa, L.J., 2006, An asymmetric hurricane wind model for storm surge and wave forecasting. AMS Annual Meeting, Atlanta.

Bausch, D., 2003, HAZUS: FEMA's GIS-based risk assessment tool. In *Proceedings of the Geospatial Information & Technology Association's 7th Annual Conference and Exhibition: A Geospatial Odyssey*. Available online at: http://gisdevelopment.net/proceedings/gita/2003/disman/dism09.shtml (accessed September 2006).

Bell, H.M. and Tobin, G.A., 2007, Efficient and effective? The 100-year flood in the communication and perception of flood risk. *Environmental Hazards*, **7**, pp. 302–311.

Blain, C.A., 1997, Modelling methodologies for the prediction of hurricane storm surge. *Recent Advances in Marine Science and Technology*, **96**, pp. 177–189.

Blain, C.A., Westerink, J.J., Luettich, R.A., 1994, The influence of domain size on the response characteristics of a hurricane storm surge model. *Journal of Geophysical Research*, **99**, pp. 467–479.

Blecic, I., Cecchini, A., Trunfio, G., 2009, A general-purpose geosimulation infrastructure for spatial decision support. *Lecture Notes in Computer Science*, **5730**, pp. 200–218.

Blog, R., 2004, A review of damage intensity scales. *Natural Hazards*, **29**, pp. 57–76.

Bocco, G., Mendoza, M., Velazquez, A., 2001, Remote sensing and GIS-based regional geomorphological mapping—a tool for land use planning in developing countries. *Geomorphology*, **39**, pp. 211–219.

Boyd, K., Hervey, R. and Stradtner, J., 2002, Assessing the vulnerability of the Mississippi Gulf Coast to coastal storms using an on-line GIS-based coastal risk atlas. In *Proceedings of the OCEANS 2002 MTS/IEEE Conference and Exhibition, 29–31 October 2002, Biloxi, MS*, pp. 1234–1240; also available online at: http://www.ncddc.noaa.gov/cra/Papers/vuln_paper (accessed 22 September 2003).

Burpee, R.W., 1972, The origin and structure of easterly waves in the lower troposphere of North Africa. *Journal of Atmospheric Science*, **29**, pp. 77–90.

Burrough, P.A., 2001, GIS and geostatistics: essential partners for spatial analysis. *Environmental and Ecological Statistics*, **8**, pp. 361–377.

Carson, T.N. and Arthur, S.T., 2000, The impact of land use-land cover changes due to urbanization on surface microclimate and hydrology: a satellite perspective. *Global and Planetary Change*, **25**, pp. 49–65.

Cattani C. and Scalia M., 2009, Wavelet analysis of spike train in the Fitzhugh model. *Lecture Notes in Computer Science*, **5730**, pp. 163–179.

Cecchini, A., 1996, Urban modelling by means of cellular automata: generalised urban automata with help on-line (AUGH) model. *Environment and Planning*, **24**, pp. 721–732.

Cecchini, A., 2006, Urban modelling by means of cellular automata generalised urban automata with help on-line (AUGH) model. *Environment and Planning*, **24**, pp. 721–732.

Center for International Earth Science Information Network (CIESIN) Columbia University and Centro Internacional de Agricultura Tropical (CIAT), 2004, Gridded Population of the World (GPW), Version 3.Columbia University, Palisades, NY. Available online at: http://beta.sedac.ciesin.columbia.edu/gpw.

Colby, J., Mulcahy, K. and Wang, Y., 2000, Modelling flooding extent from Hurricane Floyd in the coastal plains of North Carolina. *Environmental Hazards*, **2**, pp. 157–168.

Correia, F.N., Rego, F.C., Saraiva, M.G. and Ramos, I., 1998, Coupling GIS with hydrologic and hydraulic flood modelling. *Water Resources Management*, **12**, pp. 229–249.

Costa-Cabral, M., Burges, S.J., 1994, Digital Elevation Model Networks (DEMON): a model of flow over hillslopes for computation of contributing and dispersal areas. *Water Resources Research*, **30**, pp. 1681–1692.

Cruz, I.F., Sunna, W., Makar, N. and Bathala, S., 2007, A visual tool for ontology alignment to enable geospatial interoperability. *Journal of Visual Languages*, **18**, pp. 230–254.

de Longueville, M.B., 2010, Community-based geoportals: the next generation? Concept and methods for geospatial web 2.0. *Computers, Environment and Urban Systems*, **34**, pp. 299–308.

Emmons, H.W., Chang, C.T. and Watson, B.C., 2006, Taylor instability of finite surface waves. *Journal of Fluid Mechanics Digital Archive*, **10**.1017/S0022112060001420.

Farr, T.G., Rosen, P.A., Caro, E., Crippen, R., Duren, R., Hensley, S., Kobrick, M., Werner, M., Paller, M., Rodirguez, E., Roth, L., Seal, D., Shaffer, S., Shimada, J., Umland, J., Wermer M., Oskin, M., Burbank, D. and Alsdorf, D., 2007, The Shuttle Radar Topography Mission. *Reviews of Geophysics*, **45**,RG2004; DOI: 10.1029/2005RG000183.

Freeland, G.L. and Dietz, R.S., 1971, Plate tectonic evolution of Caribbean-Gulf of Mexico region. *Nature*, **232**, pp. 20–23.

Giannini, A., Kushnir, Y. and Cane, M.A., 2000, Interannual variability of Caribbean rainfall, ENSO and the Atlantic Ocean. *Journal of Climate*, **13**, pp. 297–311.

Gonnert, G., Dube, S.K., Murty, T.S. and Siefert, W., 2001, *Global Storm Surges: Theory, Observations and Applications*, edited by German Coastal Engineering Research Council, Heft 63-JAHR 2001, 623 pp.

Goodchild, M.F., Guoqing, S. and Shiren, Y., 1992, Development and test of error model for categorical data. *International Journal of Geographical Information Systems*, **6**, pp. 87–104.

Goring, D., 1999, Getting a handle on extreme sea-levels. *Aniwaniwa*,**11**, 3.

Guzman-Tapia, Y., Ramirez-Sierra, M.J., Escobedo-Ortegon, J. and Dumonteil, E., 2005, Effect of Hurricane Isidore on Triatoma dimiata distribution and Chagas disease transmission risk in the Yucatan peninsula of Mexico. *American Journal of Tropical Medicine and Hygiene*, **73**, pp. 1019–1025.

Hancock, G.R. and Evans, K.G., 2004, Channel head location and characteristics using digital elevation model. *Earth Surface Processes and Landforms*, **31**, pp. 809–824.

Hansen, M., DeFries, R., Townshend., J.G. and Sohlberg, R., 2000, Global land cover classification at 1 km resolution using a decision tree classifier. *International Journal of Remote Sensing*, **21**, pp. 1331–1365.

Hayden, M.H., Drobot, S., Radil, S., Benight, C., Gruntfest, E.C. and Barnes, L.R., 2007, Information sources for flash flood warnings in Denver, CO and Austin, TX. *Environmental Hazards*, **7**, pp. 211–219.

Holland, G.J, 1980, An analytic model of the wind and pressure profiles in hurricanes. *Monthly Weather Review*, **108**, pp. 1212–1218.

Holweg, E.J., 2000, Mariner's guide for hurricane awareness in the North Atlantic Basin. National Weather Service, United States.

Howard, R., Dodge, P., Doggett, A., Finney, J., Gurley, K., Levitan, M., Reinhold, T., Schroeder, J. and Stone, G., 2003, The landfall of Hurricane Lili in Louisiana: a summary of cooperative data collection efforts. International Conference on Wind Engineering, Lubbock, Texas.

Jenks G.F, 1967, The data model concept in statistical mapping. *International Yearbook of Cartography*, **7**, pp. 186–190.

Jenson, S.K. and Domingue, J.O., 1988, Extracting topographic structure from digital elevation data for geographic information system analysis. *Photogrammetric Engineering and Remote Sensing*, **54**, pp. 1593–1600.

Jiang, H., Halverson, J.B. and Simpson, J., 2003, Difference of rainfall distribution for tropical cyclones over land and ocean and rainfall potential derived from satellite observations and its implication on hurricane landfall flooding prediction. *Journal of Hydrometeorology*, **12** B.1.

Jones, M.T., 2003, User guide to the Centenary Edition of the GEBCO Digital Atlas and its data sets. Available online at: http://www.ngdc.noaa.gov/mgg/gebco/.

Joyce, R.J. and Ferraro, R., 2005, Improvements of CMORPH resulting from limb adjustments and normalization of AMSU-B rainfall. *Journal of Hydrometeorology*, P1.22.

Kerry, E., 2005, Increasing destructiveness of tropical cyclones over the past 30 years. *Nature*, **436**, pp. 686–688.

Klein, R.J.T., Nicholls, R.J., Thomalla, F., 2004, Resilience to natural hazards: how useful is this concept? *Environmental Hazard*, **5**, pp. 35–45.

Kok, K. and Winograd, M., 2002, Modelling land-use change for Central America, with spatial reference to the impact of hurricane Mitch. *Ecological Modelling*, **149**, pp. 53–69.

Knutson, T. R., McBride, J. L. Chan, J., Emanuel, K., Holland, G., Landsea, C., Held, I., Kossin, J.P., Srivastava, A.K. and Sugi, M., 2010, Tropical cyclones and climate change. *Nature Geoscience*, DOI: 10.1038/NGEO779.

Ledford, H., 2009, Cyberinfrastructure: feed me data. *Nature*, **459**, pp. 1047–1049.

Levizzani, V. and Mugnai, A., 2004, Rainfall measurements from space: where are we? In Proceedings of the 14th International Conference on Clouds and Precipitation, Bologna, Italy, 18–23 July 2004.

Lin, J., Ross, S.S., Sevilgen, V. and Toda, S., 2010, USGS-WHOI-DPRI Coulomb Stress-Transfer Model for the January 12, 2010, MW = 7.0 Haiti Earthquake. USGS Open-File Report 2010-1019, 7 pp.

McInnes, R.G., 2006, Responding to the Risks from Climate Change in Coastal Zones, *A good practice guide* (Ventnor: Isle of Wight Council).

McInnes, R.G., Tomalin, D. and Jakeways, J., 2000, Coastal change, climate and instability. EU Environment LIFE project (Ventnor: Isle of Wight Council).

Marghany, M., 2009, Volterra–Lax–Wendroff algorithm for modelling sea surface flow pattern from Jason-1 satellite altimeter data. *Lecture Notes in Computer Science*, **5730**, pp. 1–18.

Melelli, L. and Taramelli, A., 2004, An example of debris-flows hazard modelling using GIS. *Natural Hazard and Earth System Sciences*, **4**, pp. 347–358.

Mucher, C.A. and Badts, D.E.P.J., 2002, *Global Land Cover 2000: Evaluation of the SPOT VEGETATION sensor for land use mapping* (Wageningen: Green World Research).

Munro, A., 1999, Seeking storm surges. *New Zealand Science Monthly*, **10**, p. 11.

OCHA: OCHA Situation Report no. 2. Available online at: http://www.reliefweb.int/rw/RWB.NSF/db900SID/SNAO-6GZSTG?OpenDocument, 2005a.

OCHA: OCHA Situation Report no. 3. Available online at: http://www.reliefweb.int/rw/RWB.NSF/db900SID/EVOD-6H3DTK?OpenDocument&rc=2&emid=TC-2005-000173-SLV, 2005b.

O'Hare, G., 2001, Hurricane 07B in the Godavari delta, Andhra Pradesh, India: vulnerability, mitigation and the spatial impact. *The Geographical Journal*, **167**, pp. 23–38.

Osaragi, T., 2002, Classification methods for spatial data representation. *Centre for Advanced Spatial Analysis. Working Paper Series*, **40**, pp. 1–19.

Palmieri, S., Teodonico, L., Siani, A.M., Casale, G.R., 2006, Tropical storm impact in Central America. *Meteorological Applications*, **13**, pp. 21–28.

Pasch, R.J. and Roberts, D.P., 2006, Tropical Cyclone Report - Hurricane Stan, 1–5 October 2005, National Hurricane Center. Available online at: http://www.nhc.noaa.gov/2005atlan.shtml.

Pasqui, M., Taramelli, A., Barbour, J., Kirschbaum, D., Bottai, L., Busillo, C., Calastrini, F., Gualtieri, G., Guarnieri, F., Small, C., 2010 Dust-storm analysis in Northern China by means of advanced remote sensing analysis and atmospheric emission-dispersion modelling. *Earth Surface Process and Landforms*, submitted.

Pelupessy, W., (Ed.), 1991, *Perspectives on the Agro-export Economy in Central America* (Washington, DC: Macmillan).

Pender, G. and Neelz, S., 2007, Use of computer models of flood inundation to facilitate communication in flood risk management. *Environmental Hazards*, **7**, pp. 106–114.

Penning-Rowsell, E. (Ed.) 1996, *Improving Flood Hazard Management Across Europe* (London: Middlesex University Press).

Penning-Rowsell, E. and Fordham, M. (Eds.) 1994, *Floods across Europe. Flood Hazard Assessment, Modelling and Management* (London: Middlesex University Press).

Pielke, R.A., Jr, Rubeira, J., Landsea, C., Fernandez, M.L. and Klein, R., 2003, Hurricane vulnerability in Latin America and the Caribbean: normalised damage and loss potentials. *Natural Hazards Review*, pp. 101–114.

Pielke, R.A., Jr, Landsea, C., Mayfield, M., Laver, J. and Pasch R., 2005, Hurricanes and global warming, *Bulletin of the American Meteorological Society*, **86**, pp. 1571–1575.

Pielke, R.A., Jr, Gratz, J., Landsea, C.W., Collins, D., Saunders, M.A. and Musulin, R., 2008, Normalized hurricane damages in the United States: 1900–2005. *Natural Hazards Review*, **9**, pp. 29–42.

Puecker, T.K. and Douglas, D.H., 1975, Detection of surface-specific points by local parallel processing of discrete terrain elevation data. *Computer Graphics and Image Processing*, **4**, pp. 375–387.

Riehl, H., 1954, Tropical Meteorology (New York: McGraw-Hill).

Russel, G.L., Miller, J.R., Rind, D., Ruedy, R.A., Schmidt, G.A. and Sheth, S., 2000, Comparison of model and observed regional temperature changes during the past 40 years. *Journal of Geophysical Research*, **105**, pp. 891–898.

Saito, K., Spence, R.J.S., Going, C., Markus, M., 2004, Using high-resolution satellite images for post-earthquake building damage assessment: a study following the 26 January 2001 Gujarat earthquake. *Earthquake Spectra*, **20**, pp. 1–25.

Santini, M., Taramelli, A. and Sorichetta, A., 2010, ASPHAA: a GIS-based algorithm to calculate cell area on a latitude-longitude (geographic) regular grid. *Transactions in GIS*, **14**, pp. 351–377, DOI: 10.1111/j.1467-9671.2010.01200.x

Sanyal, J. and Lu, X.X., 2004, Application of remote sensing in flood management with special reference to monsoon Asia: a review. *Natural Hazards*, **33**, pp. 283–301.

Saunders, M., 1998, Global Warming: The view in 1998 (London: Benefield Greig Hazard Research Centre, University College London).

Scheidegger, A.E., 1994, Hazards: singularities in geomorphic systems. *Geomorphology*, **10**, pp. 19–25.

Schumann, D.A. and Partridge, W.L. (Eds.) 1989, *The Human Ecology of Tropical Land Settlement in Latin America*. Westview Special Studies on Latin America and the Caribbean (Boulder, CO: Westview Press).

Shen, B.W., Atlas, R., Reale, O., Lin, S.J., Chern, J.D., Chang, J., Henze, C. and Li, J.L., 2005, Hurricane forecasts with a global mesoscale-resolving model: preliminary results with Hurricane Katrina (2005). *Geophysical Research Letters*, **33**, L13813. DOI: 10.1029/2006GL026143.

Shipley, S.T., 2005, GIS applications in meteorology, or adventures in a parallel universe. *American Meteorological Society*, **3**, pp. 171–173.

Sorensen, J.H., 2000, Hazard warning system: review of 20 years of progress. *Natural Hazard Review*, **1**, pp. 119–125.

Speight, J.G., 1984, The role of topography in controlling through-flow generation: a discussion. *Earth Surface Processes Landforms*, **5**, pp. 187–191.

Strahler, A.N., 1980, System theory in general geography. *Physical Geography*, **1**, pp. 1–27.

Stramondo, S., Saroli, M., Tolomei, C., Moro, M., Doiumaz, F., Pesci, A., Loddo, F., Baldi, P., Boschi, E., 2007, Surface movements in Bologna (Po Plain-Italy) detected by multitemporal DInSAR. *Remote Sensing of Environment*, **110**, pp. 304–316.

Taramelli, A. and Barbour, J., 2006, A new DEM of Italy using SRTM data. *Italian Journal of Remote Sensing*, **36**, pp. 3–15.

Taramelli, A. and Melelli, L., 2007, Strategy to delineate potentially affected areas by hurricane using GIS approach. *Rend. Soc. Geol. It.*, **4**, pp. 27–34.

Taramelli, A., Melelli, L., Cattuto, C. and Gregori, G., 2008, A case of geomorphic parametrization from SRTM data. *Mem. Descr. Carta Geol. d'It.*, **LXXVIII**, pp. 289–298.

Taramelli, A. and Melelli, L., 2009a, Detecting alluvial fans using quantitative roughness characterization and fuzzy logic analysis. *Lecture Notes in Computer Science*, **5730**, pp. 251–266.

Taramelli, A. and Melelli, L., 2009b, Map of deep seated gravitational slope deformations susceptibility in central Italy derived from SRTM DEM and spectral mixing analysis of the Landsat ETM+ data. *International Journal of Remote Sensing*, **2**, pp. 357–387.

Tarboton, D.G., 1998, A new method for the determination of flow directions and upslope areas in grid digital elevation models. *Water Resources Research*, **33**, pp. 309–319.

Tarboton, D.G. and Ames, D.P., 2001, Advances in the mapping of flow networks from digital elevation data. World Water and Environmental Resources Congress, 20–24 May 2001, Orlando, Florida.

Taylor, G.I., 1950, The instability of liquid surfaces when accelerated in a direction perpendicular to their planes. In *Proceedings of the Royal Society of London Series A*, **201**, pp. 192–196.

Trenberth, K.E., Shea, D.J., 2006, Atlantic hurricanes and natural variability in 2005. *Geophysical Research Letters*, **33**.

Tucker, G.E., Catani, F., Rinaldo, A. and Bras, R.L., 2000, Statistical analysis of drainage density from digital elevation data. *Geomorphology*, **36**, pp. 187–202.

UNEP-OCHA, 2005, Hurricane Stan: Environmental Impacts from Floods and Mudslides in Guatemala – Results from a rapid environmental assessment in Guatemala. Available online at: http://ochaonline.un.org/OchaLinkClick.aspx?link=ocha&DocId=100394.

van Lynden, G.W.J. and Mantel, S., 2001, The role of GIS and remote sensing in land degradation assessment and conservation mapping: some user experiences and expectations. *International Journal of Applied Earth Observation and Geoinformation*, **3**, pp. 61–68.

Watson, C.C. and Johnson, M.E., 2005, Hurricane loss estimation models. *Bulletin of the American Meteorological Society*, pp. 1713–1726.

Webster, P.J., Holland, G.J., Curry, J.A. and Chang, H.R., 2005, Changes in tropical cyclone number, duration and intensity in a warming environment. *Science*, **309**, pp. 1844–1846.

World Bank, 1998, *World Development Indicators*, 1997, World Bank CD-ROM (Washington, DC: World Bank).

Xie, L., Bao, S., Pietrafesa, L.J., Foley, K., Fuentesa, M., 2006, Real-time hurricane surface wind forecasting model: formulation and verification. *Monthly Weather Review*, **134**, pp. 1355–1370.

Yang, C., Raskin, R., Goodchild, M., Gahegan, M., 2010, Geospatial cyberinfrastructure: past, present and future. *Computers, Environment and Urban Systems*, **34**, pp. 264–277.

Yuan, M., 2005, Beyond mapping in GIS applications to environmental analysis. *Bulletin of the American Meteorological Society*, **3**, pp. 169–170.

Zenger, A. and Smith, D.I., 2003, Impediments to using GIS for real-time disaster decision support. *Computers, Environment and Urban Systems*, **27**, pp. 23–141.

Zenger, A., Smith, D.I., Hunter, G.J., Jones, S.D., 2002, Riding the storm: a comparison of uncertainty modelling techniques for storm surge risk management. *Applied Geography*, **22**, pp. 307–330.